Supporting Information

Triazole-derivatived ligands-directed diverse structures and polyaniline-assisted capacitive performances of two new Anderson-type $[AlMo_6(OH)_6O_{18}]^{3-}$-based metal-organic complexes

Zhi-fei Zu,[#]Ju-ju Liang,[#] Zhi-han Chang*, Yu-chun Lin and Xiu-li Wang*

College of Chemistry and Materials Engineering, Bohai University, Liaoning Professional Technology Innovation Center of Liaoning Province for Conversion Materials of Solar Cell, Jinzhou 121013, P. R. China

*Corresponding authors, E-mail addresses: wangxiuli@bhu.edu.cn (Xiu-li Wang) changzhihan@bhu.edu.cn (Zhi-han Chang)

Materials and General Methods

The FT-IR spectra were taken on a Varian FT-IR 640 spectrometer (KBr pellets) in the range of 500-4000 cm^{-1}. Powder X-ray diffraction (PXRD) patterns were collected using a D/teX Ultra diffractometer with Cu Ka radiation (l = 1.5418 Å). Crystal data of complexes **1** and **2** were collected using a Bruker SMART APEXII with Mo Ka radiation (l = 0.71073 Å) system. The structures of **1** and **2** were solved by the direct method and refined by full matrix least squares on F^2 using the Olex2 software. A CHI-760 electrochemical workstation was used to measure electrochemical capacitive and collect data. The classical three-electrode system was adopted, in which the Ag/AgCl electrode was used as reference electrode and the Pt wire as the counter electrode.

Preparation of carbon paper-based electrodes modified by

complexes 1-2

The mixture of 5 mg crystal and 25 mg activated carbon was fully ground in a mortar for one hour, and then dispersed into a solution of 300 μL water and 100 μL ethanol, and sonicated for one hour to form a uniform turbid liquid. A well-dispersed slurry droplet of 10 μL was dispersed on a carbon paper electrode (0.5cm×0.5cm) and dried at room temperature for two hours. Finally, 5 μL of Nafion solution was dropped on the electrode surface and dried at room temperature.

Table.S1 Partial bond lengths and bond angles of complex **1**

1			
Zn1-N1	2.196(3)	N2-Zn1-N1	77.28(11)
Zn1-N2	2.185(3)	O2-WZn1-N2	95.80(11)
Zn1-O1W	2.064(3)	O2W-Zn1-N1	89.76(12)
Zn1-O4W	2.115(3)	O2W-Zn1-O4W	175.20(13)
Zn1-O3W	2.058(3)	O1W-Zn1-N2	164.81(11)
Zn1-O2W	2.088(3)	O1W-Zn1-O2W	90.27(14)
O3W-Zn1-N2	99.13(11)	O1W-Zn1-N1	88.87(12)
O3W-Zn1-O2W	87.16(12)	O1W-Zn1-O4W	89.86(15)
O3W-Zn1-N1	175.02(12)	O4W-Zn1-N2	85.25(12)
O3W-Zn1-O1W	95.05(12)	O4W-Zn1-N1	95.04(12)
O3W-Zn1-O4W	88.05(13)		

Symmetrycodes: [1]1-X,+Y,1/2-Z

Table.S2 Partial bond lengths and bond angles of complex **2**

2			
Zn1-O1	2.131(2)	O2W-Zn1-O1W	88.06(15)
Zn1-O3W	2.131(2)	O2W-Zn1-N2	170.43(11)
Zn1-O2W	2.064(3)	O2W-Zn1-N1	94.47(11)
Zn1-O1W	2.106(3)	O1W-Zn1-O1	88.20(12)
Zn1-N2	2.127(3)	O1W-Zn1-O3W	170.25(14)
Zn1-N1	2.137(3)	O1W-Zn1-N2	97.73(15)
O1-Zn1-O3W	86.01(9)	O1W-Zn1-N1	92.24(13)
O1-Zn1-N1	174.61(10)	N2-Zn1-O1	96.85(10)

O3W-Zn1-N1	94.26(10)	N2-Zn1-O3W	90.75(11)
O2W-Zn1-O1	90.91(11)	N2-Zn1-N1	77.77(10)
O2W-Zn1-O3W	84.20(11)		

Symmetrycodes:[1]2-X,1-Y,1-Z

Table.S3 The weak hydrogen bonding interactions of complex **1**

D - H...A	H...A	D...A	D - H...A
O(2W)-H(2WA)...O5	1.91	2.751(4)	169
O(4W)-H(4WB)...O10	1.84	2.685(4)	166

Table.S4 Hydrogen bonding interaction of complex **2**

D - H...A	H...A	D...A	D - H...A
O(3W)-H(3WB)...O11	1.89	2.730(5)	168
O(2W)-H(2WB)...O2	1.97	2.809(4)	166

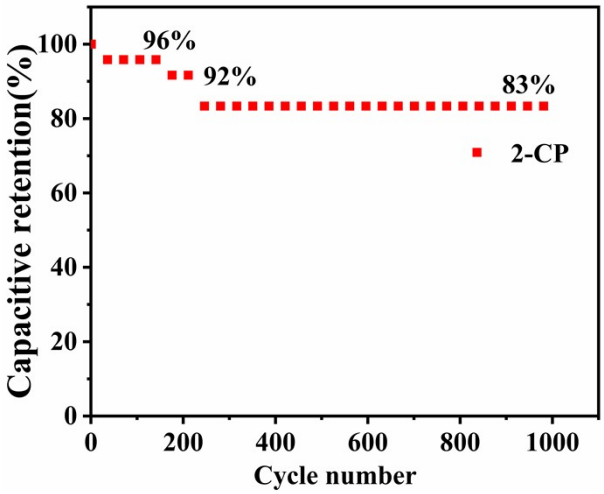

Fig. S1 The stability of capacitance following 1000 cycles at a current density of 20 $A \cdot g^{-1}$

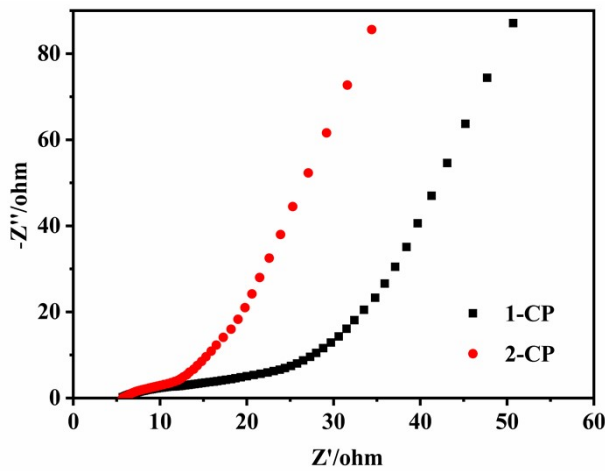

Fig. S2 Nyquist plots of complexes **1-2**

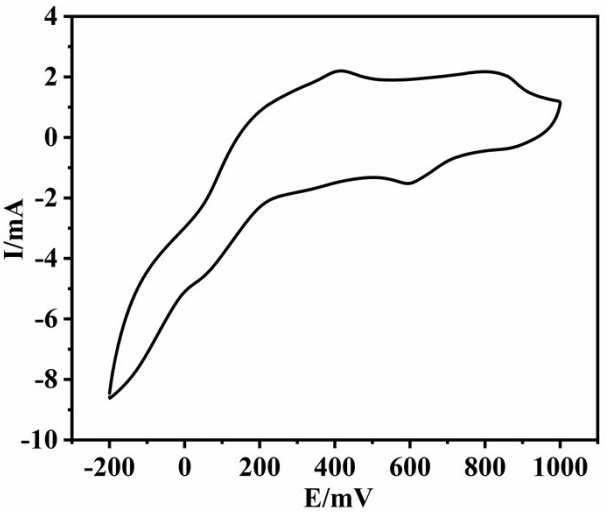

Fig. S3 The CV curves of electrochemical conditioning of PANI-**1**@**1**-CP.

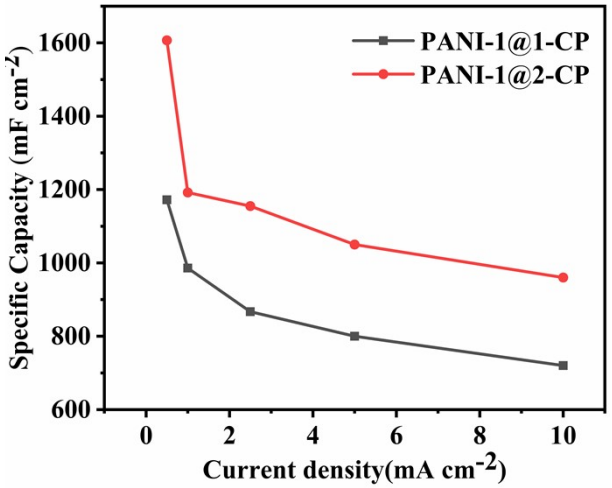

Fig. S4 The trend of areal specific capacity with current density ofPANI-**1**@**1**-CP and PANI-**1**@**2**-CP at the current densities of 0.5, 1, 2.5, 5 and 10 mA cm^{-2}.

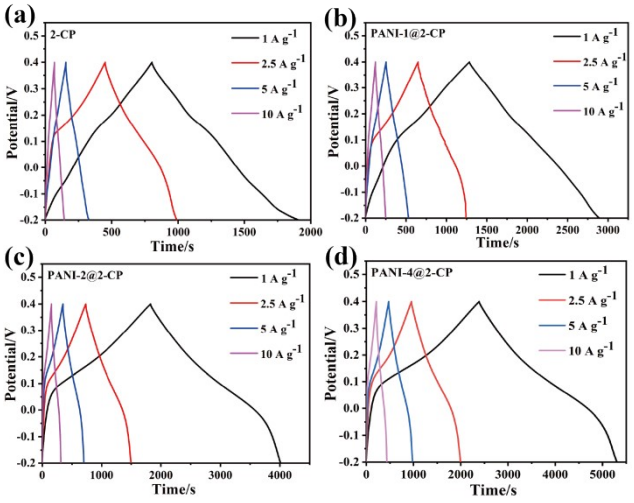

Fig. S5 The GCD curves of **2**-CP(a), PANI-**1**@**2**-CP(b), PANI-**2**@**2**-CP(c), PANI-**4**@**2**-CP(d) at the current densities of 1, 2.5, 5, 10 A g^{-1}.